Available online at www.sciencedirect.com

ScienceDirect

Procedia Structural Integrity 38 (2022) 418–427

Structural Integrity Procedia

www.elsevier.com/locate/procedia

FATIGUE DESIGN 2021, 9th Edition of the International Conference on Fatigue Design

# The Peak Stress Method applied to fatigue lifetime estimation of welded steel joints under variable amplitude multiaxial local stresses

Luca Vecchiato[1], Alberto Campagnolo[1], Beatrice Besa[1], Giovanni Meneghetti[1]*

*Department of Industrial Engineering, University of Padova, via Venezia, 1 – 35131 Padova (Italy).*

**Abstract**

Fatigue actions of most engineering welded structures involve variable amplitude (VA) loading cycles. The fatigue design of welded joints in such structures is based on the use of a fatigue strength criterion for constant amplitude (CA) loading in conjunction with a cumulative damage rule. In the present work, the Peak Stress Method (PSM), has been reformulated to estimate the lifetime of welded joints subjected to VA loadings. The PSM is an engineering finite element (FE)-oriented technique to rapidly estimate the mode I, II, and III notch stress intensity factors (NSIFs) at the weld toe or at the weld root, by taking advantage of the singular linear elastic, opening, sliding, and tearing peak stresses, respectively. Such stresses are computed at the V-notch tip by means of 2D or 3D FE models discretized using coarse meshes, provided that some conditions of applicability of the method are satisfied. The fatigue strength under CA loading is then evaluated by combining the simplicity and rapidity of the PSM in evaluating the NSIFs with a robust and validated fatigue strength criterion such as the one based on the averaged Strain Energy Density (SED), which can be written as a function of the relevant NSIFs. To preserve the simplicity of the method, its extension to VA loading conditions has been achieved by assuming the Miner's Linear Damage Rule (LDR) as a cumulative damage rule. The proposed method has been validated against new experimental results generated by testing non-load-carrying (nlc) fillet-welded joints with double inclined attachment and made of structural steel under pure axial loading.



*Keywords:* Welded Joints; Multiaxial Fatigue; Variable amplitude; Peak Stress Method; Coarse mesh

* Corresponding author. Tel.: +39 049 8276751; fax: +39 049 8276785.
*E-mail address:* giovanni.meneghetti@unipd.it


10.1016/j.prostr.2022.03.043

## 1. Introduction

The Notch Stress Intensity Factor (NSIF) based approach (Lazzarin and Tovo 1998; Lazzarin et al. 2004; Radaj et al. 2006) for the fatigue design of welded structures assumes the worst-case geometry both at the weld toe and at the weld root of the joint, consisting in a sharp V-notch having a null tip radius ($\rho = 0$) and opening angles of 135° and 0°, respectively. Then, the NSIF-parameters quantify the intensity of the singular linear elastic local stress fields. Gross and Mendelson (Gross and Mendelson 1972) defined the NSIFs according to Eq. (1).

$$K_i = \sqrt{2\pi} \cdot \lim_{r \to 0} \left[ \left( \sigma_{jk} \right)_{\theta=0} \cdot r^{1-\lambda_i} \right] \quad \text{where} \quad i=1,2,3 \quad \text{and} \quad \sigma_{jk} = \sigma_{\theta\theta}, \tau_{r\theta}, \tau_{\theta z} \ \text{respectively} \tag{1}$$

where $\lambda_i$ is the stress singularity exponent relevant to mode I, II, and III for i = 1, 2, and 3, respectively, that are functions of the V-notch opening angle 2α, while the stress components $\sigma_{\theta\theta}$, $\tau_{r\theta}$ and $\tau_{\theta z}$ are computed along the notch bisector line ($\theta = 0$ in Fig. 1a).

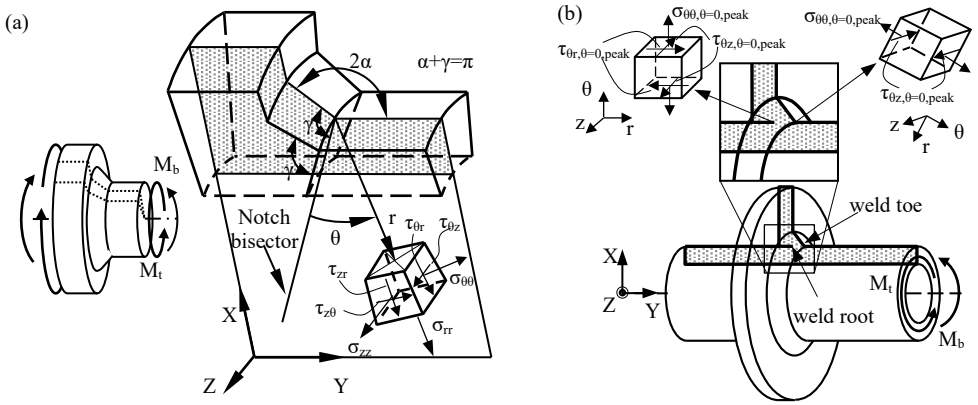


Fig. 1. (a) Polar reference system centred at the weld toe of a typical tube-to-flange welded joint geometry subjected to multiaxial bending and torsion loading. (b) Sharp V-shaped notches in a welded joint at the weld root (2α = 0°) and at the weld toe (2α ≈ 135°) sides. Definition of peak stresses $\sigma_{\theta\theta,\theta=0,peak}$, $\tau_{r\theta,\theta=0,peak}$ and $\tau_{\theta z,\theta=0,peak}$.

Lazzarin and co-workers (Lazzarin et al. 2008) proposed the average value of the strain energy density (SED) evaluated inside a material structural volume embracing the weld root or the weld toe, as a damage parameter to correlate the fatigue strength of welded components. The structural volume has been assumed as having a circular shape of radius $R_0$. When considering a general multiaxial stress state (see Fig. 1), the averaged SED can be written as a function of the ranges of the NSIF-terms, i.e., $\Delta K_1$, $\Delta K_2$, and $\Delta K_3$, through Eq. (2) (Lazzarin et al. 2008):

$$\Delta \bar{W} = \frac{e_1}{E} \left[ \frac{\Delta K_1}{R_0^{1-\lambda_1}} \right]^2 + \frac{e_2}{E} \left[ \frac{\Delta K_2}{R_0^{1-\lambda_2}} \right]^2 + \frac{e_3}{E} \left[ \frac{\Delta K_3}{R_0^{1-\lambda_3}} \right]^2 \tag{2}$$

In Eq. (2), $E$ is the material modulus of elasticity; $e_1$, $e_2$, and $e_3$ are parameters dependent on the sharp notch geometry and on the material, through the opening angle 2α and the Poisson's ratio ν, respectively (Lazzarin et al. 2008). $R_0$ is the structural volume size, which has been calibrated considering arc-welded joints made of structural steel and it was found to be 0.28 mm (Livieri and Lazzarin 2005). It should be noted that Eq. (2) is valid for welded joints loaded in the as-welded conditions, which are almost not sensitive to mean stresses according to design standards (Eurocode 3 2005). On the other hand, Eq. (2) must be modified as discussed in (Lazzarin et al. 2004; Meneghetti and Campagnolo 2020) when dealing with stress-relieved joints, to properly account for their sensitivity to mean stresses.

## 2. The Peak Stress Method (PSM)

The PSM is a numerical tool to rapidly estimate the NSIF-parameters $K_1$, $K_2$, and $K_3$ (Eq. 1), taking advantage of the opening, in-plane shear and out-of-plane shear peak stresses $\sigma_{\theta\theta,\theta=0,peak}$, $\tau_{r\theta,\theta=0,peak}$ and $\tau_{\theta z,\theta=0,peak}$, respectively. Peak stresses are referred to the V-notch bisector line (see the example in Fig. 1b) and evaluated from a linear elastic FE analysis with coarse mesh. The NSIF-terms can be estimated thanks to the PSM from the following expressions (Meneghetti and Lazzarin 2007; Meneghetti 2012, 2013):

$$K_1 \cong K^{*}_{FE} \cdot \sigma_{\theta\theta,\theta=0,peak} \cdot d^{1-\lambda_1}; \qquad K_2 \cong K^{**}_{FE} \cdot \tau_{r\theta,\theta=0,peak} \cdot d^{0.5}; \qquad K_3 \cong K^{***}_{FE} \cdot \tau_{\theta z,\theta=0,peak} \cdot d^{1-\lambda_3} \tag{3}$$

where the parameter *d* is the average size of the finite elements, which is the input parameter of the FE code before generating the free mesh. Originally, the coefficients $K^{*}_{FE}$, $K^{**}_{FE}$ and $K^{***}_{FE}$ have been calibrated by using 2D 4-node plane and 3D 8-node brick elements as summarised in (Meneghetti and Campagnolo 2020). Recently, to meet the growing demand for more efficient as well as time-saving fatigue approaches to be coupled with the 3D modelling of large-scale or even full-scale structures, the PSM has been calibrated by using 10-node tetra elements (SOLID 187 of Ansys® element library). In fact, this element type allows to efficiently discretize complex 3D joint geometries using free meshing techniques. However, the drawback of a mesh pattern made of tetra elements is its typical irregularity, so that the peak stresses could vary along the notch tip line, even though the NSIF parameters were constant. To overcome this drawback, an average peak stress value has been defined in (Campagnolo et al. 2019), smoothing the peak stress distribution along the notch tip line. More in detail, the peak stress was defined as the moving average of the peak stresses calculated on three adjacent vertex nodes; as an example, the peak stress at node n=k is computed as:

$$\overline{\sigma}_{ij,peak,n=k} = \left. \frac{\sigma_{ij,peak,n=k-1} + \sigma_{ij,peak,n=k} + \sigma_{ij,peak,n=k+1}}{3} \right|_{n=node} \tag{4}$$

Therefore, the PSM-coefficients $K^{*}_{FE}$, $K^{**}_{FE}$, and $K^{***}_{FE}$ have been calibrated by adopting 10-node tetra elements (SOLID 187 of Ansys® library) and by rewriting Eq. (3) using the average peak stresses according to Eq. (4). It is worth recalling that the PSM based on 10-node tetra elements should not be applied at nodes laying on a free surface of the analysed structure, since the peak stresses at those nodes are influenced by the distorted mesh pattern. Moreover, the peak stresses must be calculated only at the vertex nodes of 10-node tetra elements, while the peak stresses calculated at mid-side nodes must be neglected. The results obtained from the calibration of the 3D-PSM based on 10-node tetra elements (Campagnolo et al. 2019) are summarised in Table 1, along with the minimum mesh density ratios *a/d, a* being the characteristic size of the considered sharp V-notch, which guarantee the convergence of the PSM parameters $K^{*}_{FE}$, $K^{**}_{FE}$, and $K^{***}_{FE}$, respectively.

Table 1. Summary of parameters $K^{*}_{FE}$, $K^{**}_{FE}$ and $K^{***}_{FE}$ and mesh density *a*/*d* requirements to apply the PSM with Ansys® (Campagnolo et al. 2019; Meneghetti and Campagnolo 2020). n.a. = not applicable

| Loading | FE analysis | | PSM parameters | 2α = 0° | 2α = 90° | 2α = 120° | 2α = 135° | *a* – weld root° | *a* – weld toe° |
|---|---|---|---|---|---|---|---|---|---|
| | | FE type# | | | | | | | |
| Mode I | 3D+ | Tetra-10 | $K^{*}_{FE}$ $(a/d)_{min}$ | 1.05±15% 3 | 1.05±15% 3 | 1.05±15% 3 | 1.21±10% 1 | min{*l*, *z*} | *t* |
| Mode II | 3D+ | Tetra-10 | $K^{**}_{FE}$ $(a/d)_{min}$ | 1.63±20% 1 | 2.65±10% 1 | n.a. n.a. | n.a. n.a. | min{*l*, *z*} | n.a. |
| Mode III | 3D+ | Tetra-10 | $K^{***}_{FE}$ $(a/d)_{min}$ | 1.37±15% 3 | 1.37±15% 3 | 1.70±10% 3 | 1.70±10% 3 | min{*l*, *z*} | *t* |

+ 'Full graphics' option must be activated when calculating peak stresses according to 3D PSM
# FE of Ansys® code: Tetra 10 = SOLID 187
° *l*, *z*, *t* have been defined in (Meneghetti and Campagnolo 2020)

### 2.1. Fatigue design of welded joints under constant amplitude (CA) loading according to the PSM

Equation (2) shows that the averaged SED can be expressed as a function of NSIF-terms $K_1$, $K_2$, and $K_3$, which the PSM readily estimates thanks to Eq. (3). Therefore, the averaged SED can be rewritten as a function of the average peak stresses defined by Eq. (4). After that, an equivalent uniaxial plane strain state can be introduced so as $W = \left(1-\nu^2\right)\sigma_{eq,peak}^2 / 2E$ to define an equivalent peak stress generating the same local SED (Meneghetti et al. 2017):

$$\Delta\sigma_{eq,peak} = \sqrt{f_{w1}^2 \cdot \Delta\overline{\sigma}_{\theta\theta,\theta=0,peak}^2 + f_{w2}^2 \cdot \Delta\overline{\tau}_{r\theta,\theta=0,peak}^2 + f_{w3}^2 \cdot \Delta\overline{\tau}_{\theta z,\theta=0,peak}^2} \quad \text{where } f_{wi} = K_{FE} \cdot \sqrt{\frac{2e_i}{1-\nu^2}} \cdot \left(\frac{d}{R_0}\right)^{1-\lambda_i} \quad i=1,2,3 \tag{5}$$

where the coefficients $f_{wi}$ (i = 1, 2, 3 is the loading mode) take into account the stress averaging inside the material-structural volume having size $R_0 = 0.28$ mm for steel joints. Equations (3) and (5) highlight that both peak stresses and parameters $f_{wi}$ depend on the average finite element size $d$ adopted to generate the free mesh pattern; on the other hand, the equivalent peak stress defined in Eq. (5) is independent of the FE size $d$, thanks to the multiplication of the peak stresses by the relevant $f_{wi}$ parameters. It is worth recalling that when the weld toe is under investigation, the mode II stress field is always non-singular since $2\alpha \cong 135° > 102°$, therefore the relevant contribution in Eq. (5) becomes null.

In a recent review of the PSM (Meneghetti and Campagnolo 2020), a criterion has been proposed to select the appropriate curve for the fatigue design of arc-welded joints made of structural steel. It is based on the relative SED contributions due to mode II/III shear stresses and mode I normal stresses. Accordingly, a local biaxiality ratio $\lambda$ has been defined and expressed as a function of the peak stresses as follows:

$$\lambda = \frac{f_{w2}^2 \cdot \Delta\overline{\tau}_{r\theta,\theta=0,peak}^2 + f_{w3}^2 \cdot \Delta\overline{\tau}_{\theta z,\theta=0,peak}^2}{f_{w1}^2 \cdot \Delta\overline{\sigma}_{\theta\theta,\theta=0,peak}^2} \tag{6}$$

Equation (6) delivers $\lambda = 0$ for a pure local mode I stress state, $\lambda \to \infty$ for a pure local mode II+III shear stress state and $\lambda$ in the range from 0 to $\infty$ when a mixed mode opening-shear stress condition is present. The criterion for selecting the proper fatigue design curve was provided in (Meneghetti and Campagnolo 2020) as a function of $\lambda$ (Eq. (6)) for welded steels and aluminium alloys and it has been summarised in Table 2 for the former materials, which includes also the relevant endurable stresses and slopes of the master curves.

Table 2: Criterion for selecting the reference PSM-based fatigue design curve for arc-welded joints

| Class of materials | T (mm) | $\lambda$ Eq. (6), (10) | $\Delta\sigma_{eq,peak,A,50\%}$ (MPa) | $\Delta\sigma_{eq,peak,A,97.7\%}$ (MPa) | k | $T_\sigma$ |
|---|---|---|---|---|---|---|
| Structural steels | $T \geq 2$ mm | $\lambda = 0$ | 214 | 156 | 3 | 1.90 |
| | $T \geq 2$ mm | $\lambda > 0$ | 354 | 257 | 5 | 1.90 |

### 2.2. Fatigue design of welded joints under variable amplitude (VA) loading according to the PSM

In the present work, the previous expressions (5) and (6) are extended to the case of welded joints subjected to variable amplitude (VA) fatigue loading conditions. First of all, the load history of each peak stress component $\sigma_{\theta\theta,\theta=0,peak}(t)$, $\tau_{r\theta,\theta=0,peak}(t)$ and $\tau_{\theta z,\theta=0,peak}(t)$ must be derived at each FE node of the weld toe or root side by means of a FE analysis according to PSM. Then, a cycle counting method (e.g., rainflow) must be applied to each load history $\sigma_{\theta\theta,\theta=0,peak}(t)$, $\tau_{r\theta,\theta=0,peak}(t)$ and $\tau_{\theta z,\theta=0,peak}(t)$ to derive the load levels of each peak stress component in terms of stress range and number of loading cycles, i.e. $[(\Delta\sigma_{\theta\theta,\theta=0,peak})_i,(n_I)_i]$, $[(\Delta\tau_{r\theta,\theta=0,peak})_j,(n_{II})_j]$, $[(\Delta\tau_{\theta z,\theta=0,peak})_h,(n_{III})_h]$. The number of load levels for mode I, II, and III loadings are defined as $n_{\sigma I}$, $n_{\tau II}$ and $n_{\tau III}$, respectively, while the total number of cycles of each loading mode is defined as the sum of the number of cycles of each load level, i.e. $(n_I)_{tot}=\Sigma(n_I)_i$, $(n_{II})_{tot}=\Sigma(n_{II})_j$ e $(n_{III})_{tot}=\Sigma(n_{III})_h$, these values being correlated to the physical reference duration of the analysed load history. It is useful to define $n_0 = \min\{(n_I)_{tot},(n_{II})_{tot},(n_{III})_{tot}\}$. In the example of Fig. 2a,b,c, it is assumed $n_0 = (n_{II})_{tot}$. After that, the equivalent peak stress for each load level can be calculated by the following equations, which have been derived from Eq. (5) with reference to a single loading mode:

$$\left(\Delta\sigma_{eq,peak,I}\right)_i = \sqrt{f_{w1}^2 \cdot \left(\Delta\bar{\sigma}_{\theta\theta,\theta=0,peak}\right)_i^2}\ ;\ \left(\Delta\sigma_{eq,peak,II}\right)_j = \sqrt{f_{w2}^2 \cdot \left(\Delta\bar{\tau}_{r\theta,\theta=0,peak}\right)_j^2}\ ;\ \left(\Delta\sigma_{eq,peak,III}\right)_h = \sqrt{f_{w3}^2 \cdot \left(\Delta\bar{\tau}_{\theta z,\theta=0,peak}\right)_h^2} \quad (7)$$

Then, the Palmgren-Miner linear-damage rule must be applied, separately for each loading mode (see Fig. 2a,b,c), to derive an equivalent peak stress which generates the same damage of the $n$ load levels (i.e. $n_{\sigma I}$, $n_{\tau II}$ and $n_{\tau III}$) previously defined, but by acting for $n_0$ cycles, i.e. the same number of cycles for all loading modes. To do so, the PSM master curve valid for the considered loading mode is adopted according to Table 2, e.g. when dealing with steel welded joints under mode I loading ($\lambda = 0$), the inverse slope is $k_1 = 3$, while under mode II and mode III ($\lambda \to \infty$) the inverse slopes are $k_2 = k_3 = 5$ (Table 2):

$$\Delta\sigma_{eq,peak,I} = \left[\sum_{i=1}^{n_{\sigma I}} \frac{(n_I)_i}{n_0} \left(\Delta\sigma_{eq,peak,I}\right)_i^{k_1}\right]^{\frac{1}{k_1}};\ \Delta\sigma_{eq,peak,II} = \left[\sum_{j=1}^{n_{\tau II}} \frac{(n_{II})_j}{n_0} \left(\Delta\sigma_{eq,peak,II}\right)_j^{k_2}\right]^{\frac{1}{k_2}};\ \Delta\sigma_{eq,peak,III} = \left[\sum_{h=1}^{n_{\tau III}} \frac{(n_{III})_h}{n_0} \left(\Delta\sigma_{eq,peak,III}\right)_h^{k_3}\right]^{\frac{1}{k_3}} \quad (8)$$

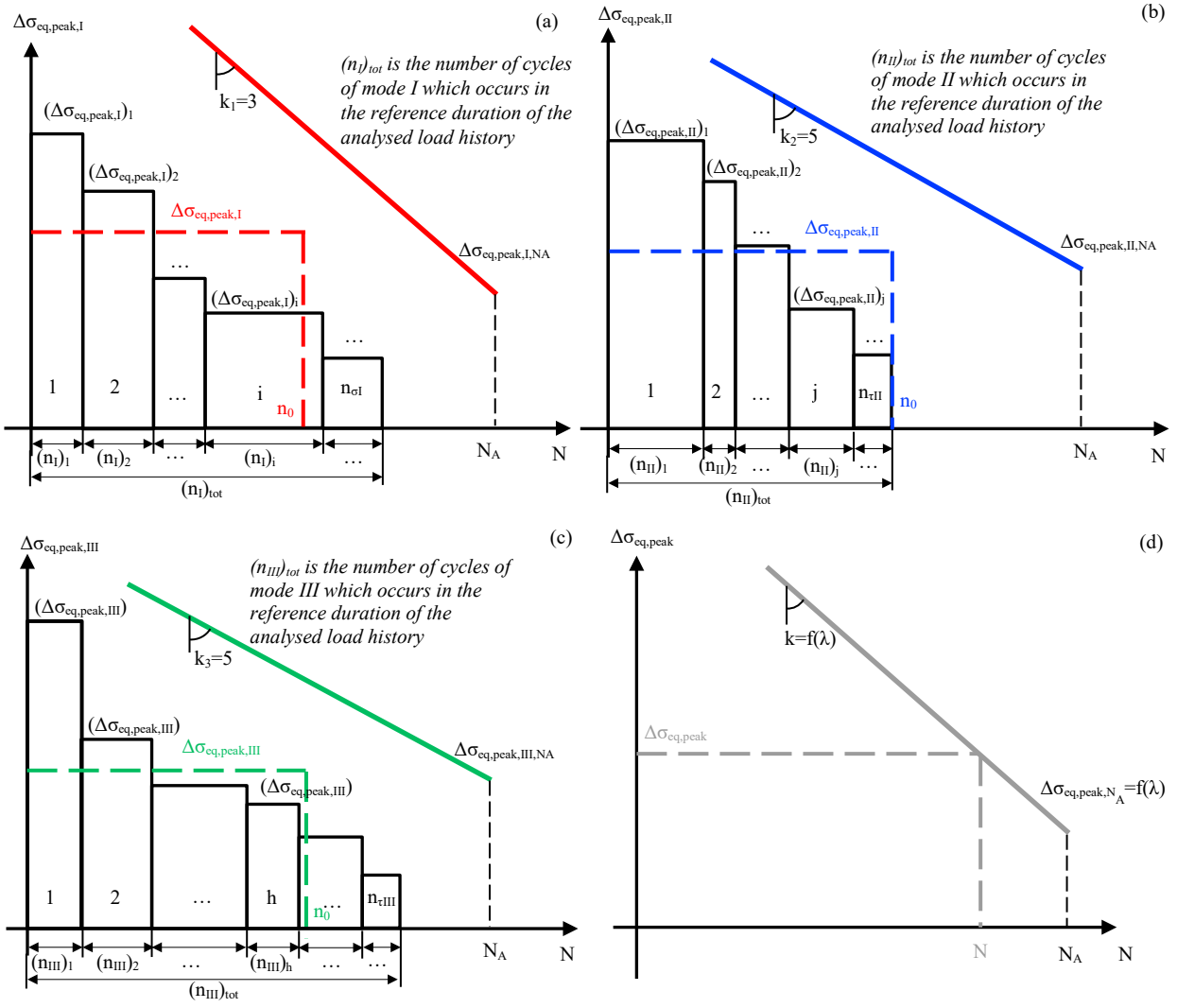


Fig. 2. Palmgren-Miner linear-damage rule applied to derive an equivalent peak stress which generates the same damage of the n load levels (i.e. $n_{\sigma I}$, $n_{\tau II}$ and $n_{\tau III}$), but by acting for $n_0$ cycles for: (a) mode I, (b) mode II and (c) mode III contributions. (d) Overall equivalent peak stress compared with the proper design curve to estimate the fatigue life of the considered welded joint under VA loading conditions.

Once calculated the equivalent peak stresses for all loading modes (Fig. 2a,b,c), the overall equivalent peak stress and the local biaxiality ratio can be derived by Eqs. (9) and (10) and adopted to estimate the fatigue life of the considered welded joint under VA loading condition (see Fig. 2d).

$$\Delta\sigma_{eq,peak} = \sqrt{\Delta\sigma^2_{eq,peak,I} + \Delta\sigma^2_{eq,peak,II} + \Delta\sigma^2_{eq,peak,III}} \tag{9}$$

$$\lambda = \frac{\Delta\sigma^2_{eq,peak,II} + \Delta\sigma^2_{eq,peak,III}}{\Delta\sigma^2_{eq,peak,I}} \tag{10}$$

## 3. Experimental Validation

### *3.1. Fatigue Tests*

The tested joints were non-load-carrying (nlc) fillet-welded joints with double inclined attachment made of a 8 mm thick S355 steel plate (see Fig. 3a). This joint geometry has been chosen because it allows to apply an in-phase multiaxial stress state at the weld toe through a uniaxial test machine. Accordingly, all specimens were tested in the as-welded state under pulsating loading (R = 0.05) by means of an MFL axial servo-hydraulic machine, with a load capacity of 250 kN and equipped with an MTS TestStar IIm digital controller.

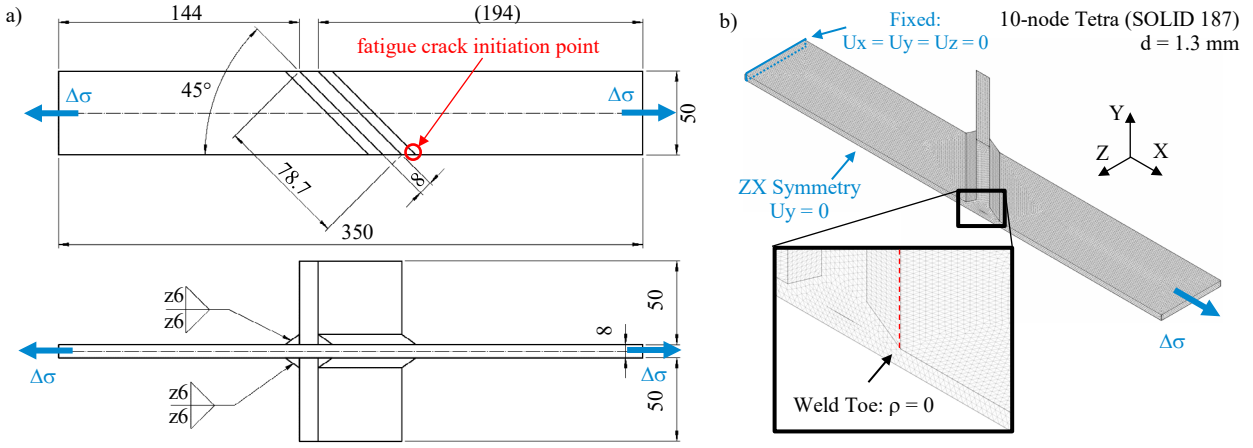


Fig. 3. Tested specimens (dimensions are in mm): (a) joint geometry and loading conditions; (b) FE analysis for fatigue lifetime estimation according to the PSM.

All tests were carried out both under constant (CA) and variable amplitude (VA) loading adopting the p-type spectrum (Hobbacher 1977) reported in Fig. 4. The cycles distribution of the p-type spectrum is derived from that of a stationary zero-mean narrow-band Gaussian random process $\{\sigma(t)\}$. More in detail, it has been demonstrated that the probability density function of peaks, and of troughs for symmetry reasons, of a stationary zero-mean Gaussian random process $\{\sigma(t)\}$ follows the Rice distribution and is a function of the bandwidth of the process (Rice 1944). In case the stationary zero-mean Gaussian random process is a narrow-band process, the probability density function of peaks (and troughs) can be simplified into a Rayleigh distribution and turns out to be equal to the probability density function of stress amplitudes $\sigma_a$:

$$p(\sigma_a) = \frac{\sigma_a}{rms^2} e^{-\frac{1}{2}\left(\frac{\sigma_a}{rms}\right)^2} \tag{11}$$

where $rms$ is the Root Mean Square stress value of the random process. Accordingly, the number of exceeding cycles N of a stationary zero-mean narrow-band Gaussian random process can be obtained from the complementary cumulative distribution function, or exceedance, of the Rayleigh distribution:

$$\frac{N}{N_0} = 1 - \int_0^{\sigma_a} p(\xi)d\xi = \int_{\sigma_a}^{\infty} p(\xi)d\xi = e^{-\frac{1}{2}\left(\frac{\sigma_a}{rms}\right)^2} \tag{12}$$

where N is the exceedance number of cycles, i.e. the number of cycles whose stress amplitude is higher than or equal to $\sigma_a$ and $N_0$ is the total number of cycles, i.e. the length of the spectrum. Theoretically the Rayleigh distribution is defined for values ranging from 0 to infinity, but in practice peaks do not exceed a certain value of $\sigma_a/rms$ called clipping ratio. Haibach et al. (Haibach et al. 1976) proposed to set the number of exceeding cycles N of the maximum stress level (clipping ratio) equal to one (in other words this means that the highest stress level is applied only once in the spectrum). Consequently, the clipping ratio becomes a function of the length of the spectrum according to Eq. (13).

$$\frac{1}{N_0} = e^{-\frac{1}{2}\left(\frac{\sigma_{a,\max}}{rms}\right)^2} \quad \rightarrow \quad \frac{\sigma_{a,\max}}{rms} = \sqrt{2\ln N_0} \quad \rightarrow \quad rms = \frac{\sigma_{a,\max}}{\sqrt{2\ln N_0}} \tag{13}$$

By substituting the $rms$ value from Eq. (13) into Eq. (12), the number of exceeding cycles N can be rewritten as a function of the relative stress amplitudes $\sigma_a/\sigma_{a,max}$ or of the relative stress ranges $\Delta\sigma/\Delta\sigma_{max}$ as reported in Eq. (14) (Gaßner et al. 1964; Hanke 1970; Heuler et al. 2005):

$$N = e^{\left[1 - \left(\frac{\Delta\sigma}{\Delta\sigma_{\max}}\right)^2\right]\ln N_0} \tag{14}$$

In the present work, the length of the spectrum has been fixed to $N_0 = 10^4$ cycles (Fig. 4).

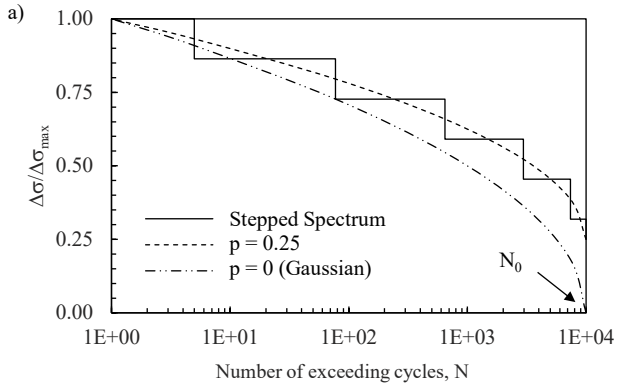


b)

| Δσ/Δσmax [-] | n [cycles] | N [cycles] |
|---|---|---|
| 1.000 | 5 | 5 |
| 0.864 | 72 | 77 |
| 0.727 | 569 | 646 |
| 0.591 | 2313 | 2959 |
| 0.455 | 4416 | 7375 |
| 0.318 | 2625 | 10000 |

Fig. 4. Stress range spectrum: (a) comparison between a standard Gaussian spectrum (p = 0), a p-type spectrum with p = 0.25, and the applied stepped spectrum; (b) the applied relative nominal stress ranges $\Delta\sigma/\Delta\sigma_{max}$ with their corresponding number of cycles n and exceeding cycles N.

Then, once the exceedance cycle distribution is known, to obtain the p-type spectrum the amplitude of the stress ranges of the Gaussian spectrum (p = 0) has to be amplified by substituting p = 0.25 into the following expression (Gurney 2006):

$$\left(\frac{\Delta\sigma}{\Delta\sigma_{max}}\right)_p = p + (1-p)\left(\frac{\Delta\sigma}{\Delta\sigma_{max}}\right)_{Gaussian,\,p=0} \quad \text{where} \quad p = \frac{\Delta\sigma_{min}}{\Delta\sigma_{max}} \tag{15}$$

In this work, the obtained p-type spectrum has been discretized in six steps (Fig. 4) and applied in a decreasing/decreasing sequence until failure. The spectrum was discretized with so few steps to allow the test equipment to correctly apply load levels while avoiding transients from one load level to another as much as possible. For the same reason, loads have been applied with a frequency between 0.1 and 10 Hz, depending on their level.

A total of 9 specimens, 5 under CA loading and 4 under VA loading, have been tested. In all specimens, fatigue cracks initiated at the weld toe on the plate's side and then propagated through the thickness and through the width, as shown in Fig. 5. The number of cycles to failure $N_f$ has been recorded and the fatigue test interrupted when the fatigue crack reached roughly half the plate thickness in length. In case no fatigue cracks were detected, $2 \cdot 10^6$ cycles were defined as runout. The Whoeler curve for CA data and the Gassner curve for VA data are reported in Fig. 6 in which fatigue tests results are expressed in terms of number of cycles to failure versus the maximum applied nominal stress range $\Delta\sigma_{max}$. The reported scatter bands have been fitted on experimental data and refer to survival probabilities of 2.3% and 97.7% with a confidence level of 95%.

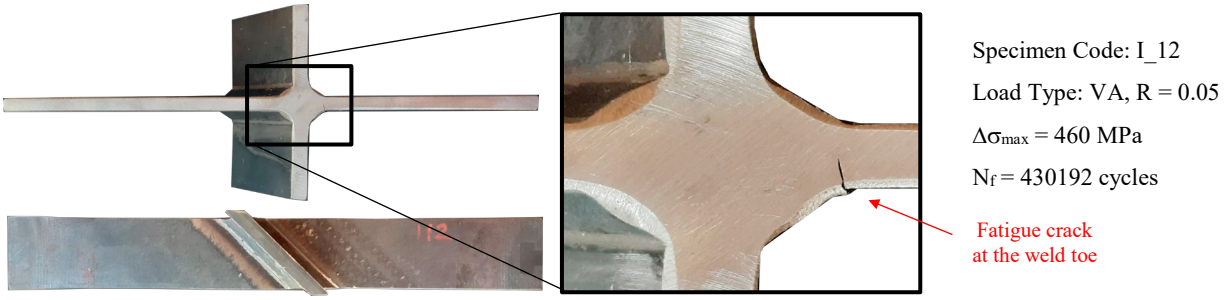


Fig. 5. Fatigue crack initiation point: example of crack at failure observed in specimen I_12, tested under VA loading.

## 4. Fatigue strength assessment according to the PSM

In the present manuscript, the experimental fatigue results have been analysed by means of the 3D-PSM procedure discussed in Section 2. Accordingly, a 3D FE analysis of the welded joint has been performed assuming a sharp V-notch at the weld toe ($\rho = 0$) with an opening angle $2\alpha = 135°$. As shown in Fig. 3b, only half of the welded joint was modelled using the ZX plane of symmetry. A free mesh pattern of tetrahedral 10-node elements (SOLID 187 of Ansys® element library) has been generated adopting a 'global element size' complying with the conditions of applicability of the PSM: the 'global element size' $d$ has been imposed equal to $a/3 = 4/3 \approx 1.3$ mm, the required mesh density ratio being $a/d \geq 3$ (see Table 1) and the characteristic size being equal to half the plate thickness for the weld toe ($a = 8/2 = 4$ mm). After having solved the model, the peak stresses $\sigma_{\theta\theta,\theta=0,peak}$ and $\tau_{\theta z,\theta=0,peak}$ have been extrapolated along the weld toe line and the corresponding average values $\overline{\sigma}_{\theta\theta,\theta=0,peak}$ and $\overline{\tau}_{\theta z,\theta=0,peak}$ have been calculated according to Eq. (4). Then, the equivalent peak stress for each load level has been calculated both for CA and VA loadings by following the procedure explained in sections 2.1 and 2.2, respectively. Their distributions are reported as a function of the normalized curvilinear coordinate $s/s_{max}$ along the weld toe line in Fig. 7a. Noteworthily, the PSM exactly estimates the crack initiation point: the maximum value of the equivalent peak stress occurs at point B for both CA and VA loadings (see Fig.7a), i.e. at the experimental crack initiation location. Accordingly, the value of the equivalent peak stress at point B has been adopted to estimate the fatigue lifetime of the tested specimens. The result of this analysis is shown in Fig. 7b, which reports the fatigue test results expressed in terms of number of cycles to failure as a function of the range of the equivalent peak stress evaluated at the fatigue crack initiation point (Point B in Fig. 7a).

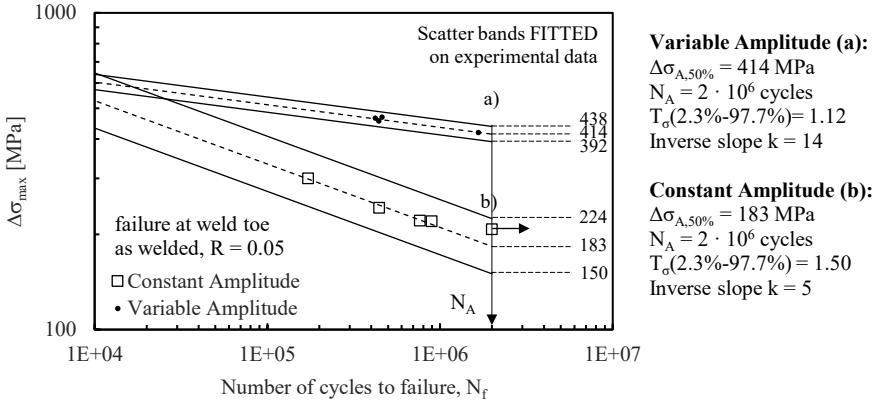


Fig. 6. Results of experimental fatigue tests performed on non-load-carrying (nlc) fillet-welded joints with double inclined attachment expressed in terms of nominal stress range: (a) the Whoeler curve of the CA loading and (b) the Gassner curve of the VA loading.

Figure 7b also includes for comparison the PSM-based fatigue design scatter band calibrated on fatigue data generated from steel welded joints subjected to pure mode III loading (Meneghetti 2013) (k=5), which has been selected because of a computed local biaxiality ratio λ greater than zero (λ = 1.90 for CA and λ = 2.13 for VA). Interestingly, it can be observed from Fig. 7b that all experimental results fall inside the PSM-based scatter band, which has not been fitted on the fatigue results of the present paper.

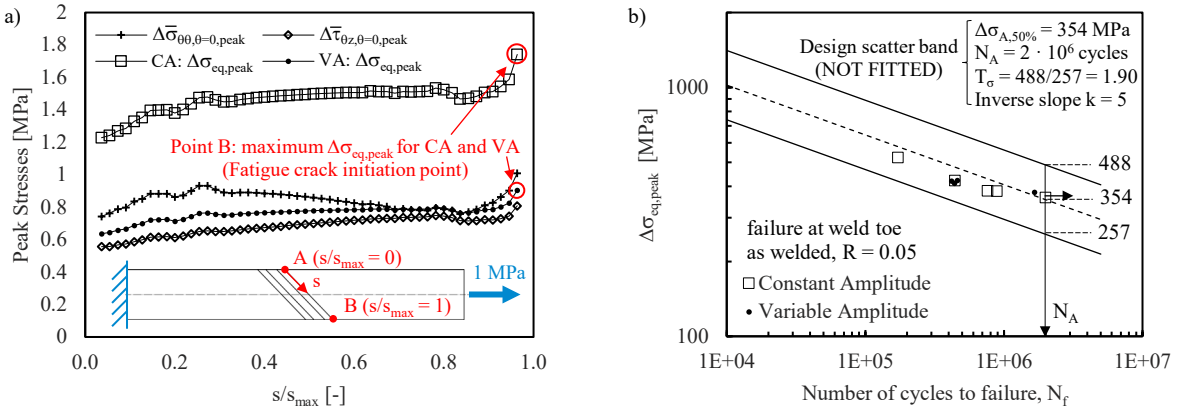


Fig. 7. Fatigue lifetime estimation according to the PSM. (a) FE analysis results: distributions of mode I peak stress range $\Delta\bar{\sigma}_{\theta\theta,\theta=0,peak}$, mode III peak stress range $\Delta\bar{\tau}_{\theta\theta,\theta=0,peak}$ and equivalent peak stress ranges $\Delta\sigma_{eq,peak}$ for both CA and VA loading along the weld toe line; (b) synthesis of the experimental fatigue results in terms of number of cycles to failure as a function of the range of the equivalent peak stress at point B.

## 5. Conclusions

In the present paper, the Peak Stress Method has been extended for the first time to steel welded joints in the as-welded state subjected to multiaxial and Variable Amplitude (VA) fatigue loadings. Basically, the fatigue strength assessment under Constant Amplitude (CA) loading is performed by combining the simplicity and rapidity of the PSM in evaluating the NSIFs by means of FE analyses with a robust and validated fatigue strength criterion such as the one based on the averaged Strain Energy Density (SED), which can be written as a function of the relevant NSIFs. To preserve the simplicity of the method, its extension to VA loading conditions has been achieved by assuming the Palmgren-Miner's Linear Damage Rule (LDR) as cumulative damage rule.

The capability and validity of the proposed method have been verified against new experimental results generated by fatigue testing non-load-carrying (nlc) fillet-welded joints with double inclined attachment and made of structural steel. The chosen geometry was adopted for generating an in-phase local multiaxial stress state at the weld toe through a uniaxial test machine. The welded joints were tested in the as-welded conditions both under CA and VA loadings. In the latter case, a p-type spectrum has been adopted and applied as a block program. Finally, the obtained fatigue results have been analyzed according to the proposed approach, obtaining a good agreement between theoretical estimations and experimental fatigue results.

## References

Campagnolo A, Roveda I, Meneghetti G (2019) The Peak Stress Method combined with 3D finite element models to assess the fatigue strength of complex welded structures. Procedia Struct Integr 19:617–626. https://doi.org/10.1016/j.prostr.2019.12.067

Eurocode 3 (2005) Design of steel structures – part 1–9: Fatigue. CEN

Gaßner E, Griese FW, Haibach E (1964) Ertragbare Spannungen und Lebensdauer einer Schweißverbindung aus Stahl St 37 bei verschiedenen Formen des Beanspruchungskollektivs. Arch für das Eisenhüttenwes 35:255–267. https://doi.org/10.1002/srin.196402317

Gross B, Mendelson A (1972) Plane elastostatic analysis of V-notched plates. Int J Fract Mech 8:267–276. https://doi.org/10.1007/BF00186126

Gurney T (2006) Cumulative Damage of Welded Joints. Woodhead Publishing

Haibach E, Fisher R, Schutz W, Huck M (1976) A standard random load sequence of Gaussian type recommended for general application in fatigue testing; its mathematical background and digital generation. SEE Conf Fatigue Test Des 2:

Hanke M (1970) Eine Methode zur Beschreibung der Betriebslastkollektive als Grundlage für Betriebsfestigkeitsversuche. ATZ Automob Zeitschrift 72:91–97

Heuler P, Bruder T, Klätschke H (2005) Standardised load-time histories - A contribution to durability issues under spectrum loading. Materwiss Werksttech 36:669–677. https://doi.org/10.1002/mawe.200500936

Hobbacher A (1977) Cumulative Fatigue by Fracture Mechanics. J Appl Mech 44:769–771. https://doi.org/10.1115/1.3424173

Lazzarin P, Livieri P, Berto F, Zappalorto M (2008) Local strain energy density and fatigue strength of welded joints under uniaxial and multiaxial loading. Eng Fract Mech 75:1875–1889. https://doi.org/10.1016/j.engfracmech.2006.10.019

Lazzarin P, Sonsino CM, Zambardi R (2004) A notch stress intensity approach to assess the multiaxial fatigue strength of welded tube-to-flange joints subjected to combined loadings. Fatigue Fract Eng Mater Struct 27:127–140. https://doi.org/10.1111/j.1460-2695.2004.00733.x

Lazzarin P, Tovo R (1998) A notch intensity factor approach to the stress analysis of welds. Fatigue Fract Eng Mater Struct 21:1089–1103. https://doi.org/10.1046/j.1460-2695.1998.00097.x

Livieri P, Lazzarin P (2005) Fatigue strength of steel and aluminium welded joints based on generalised stress intensity factors and local strain energy values. Int J Fract 133:247–276. https://doi.org/10.1007/s10704-005-4043-3

Meneghetti G (2012) The use of peak stresses for fatigue strength assessments of welded lap joints and cover plates with toe and root failures. Eng Fract Mech 89:40–51. https://doi.org/10.1016/j.engfracmech.2012.04.007

Meneghetti G (2013) The peak stress method for fatigue strength assessment of tube-to-flange welded joints under torsion loading. Weld World 57:265–275. https://doi.org/10.1007/s40194-013-0022-x

Meneghetti G, Campagnolo A (2020) State-of-the-art review of peak stress method for fatigue strength assessment of welded joints. Int J Fatigue 139:105705. https://doi.org/10.1016/j.ijfatigue.2020.105705

Meneghetti G, Campagnolo A, Rigon D (2017) Multiaxial fatigue strength assessment of welded joints using the Peak Stress Method – Part II: Application to structural steel joints. Int J Fatigue 101:343–362. https://doi.org/10.1016/j.ijfatigue.2017.03.039

Meneghetti G, Lazzarin P (2007) Significance of the elastic peak stress evaluated by FE analyses at the point of singularity of sharp V-notched components. Fatigue Fract Eng Mater Struct 30:95–106. https://doi.org/10.1111/j.1460-2695.2006.01084.x

Radaj D, Sonsino CM, Fricke W (2006) Fatigue Assessment of Welded Joints by Local Approaches, 2nd edn. Woodhead Publishing, Cambridge

Rice SO (1944) Mathematical Analysis of Random Noise. Bell Syst Tech J 23:282–332. https://doi.org/10.1002/j.1538-7305.1944.tb00874.x